Atmospheric Research 315 (2025) 107912

Contents lists available at ScienceDirect

Atmospheric Research

journal homepage: www.elsevier.com/locate/atmosres

Future winter snowfall and extreme snow events in the Pyrenees

Josep Bonsoms [a,*], Juan I. López-Moreno [b], Marc Lemus-Cánovas [c,d], Marc Oliva [a]

[a] Department of Geography, Universitat de Barcelona, Barcelona, Spain
[b] Instituto Pirenaico de Ecología (IPE-CSIC), Campus de Aula Dei, Zaragoza, Spain
[c] Eurac Resarch, Bolzano, Italy
[d] CRETUS Institute, Nonlinear Physics Group, Faculty of Physics, Universidade de Santiago de Compostela, Galicia, Spain

ARTICLE INFO

Keywords:
Snowfall
Climate change
Mountain climate
Pyrenees

ABSTRACT

Snowfall is a crucial climate variable in mountainous regions: it influences hydrological and ecosystem dynamics and has a major impact on socioeconomic activities. This study examines the future changes (2024 to 2100) in winter (December, January and February, included) snowfall and extreme snow events in the Pyrenees, using a high-resolution dataset (2.5 km) derived from multiple CMIP5 General Circulation Models (GCMs) under RCP4.5 and RCP8.5 greenhouse gas scenarios, forced with the SAFRAN model. Winter snowfall shifts are examined considering accumulated snowfall (SF), extreme snowfall (Percentile >95th; SF95) per season, and return period levels (RPs) based on fitting Generalized Extreme Value to annually maximum SF. The data indicate an overall decline in SF across the entire mountain range and at all elevations. Trend analysis reveals a statistically significant negative evolution of SF (Tau Mann-Kendall >0.3; *p*-value ≤0.05) for most of the mountain range under RCP8.5. Projections for the end of the 21st century (2080–2100 period) anticipate reductions ranging from −9 % (RCP4.5; 2500–3000 m) to −29 % (RCP8.5; 1000–1500 m) compared to the historical climate (1960–2006 period). SF95 projections range from +2 % (RCP4.5; 2500–3000 m) to −25 % (RCP8.5; 2500–3000 m) for the same periods. Annual maximum extreme snowfall RPs indicate decreases over the historical period, regardless of the scenario and elevation range. These changes are attributed to warming and declining precipitation (P), with maximum P reductions reaching reduction of −24 % for RCP8.5 (2080–2100 period). Differences among GCMs contribute to a variability of ±20 % around the average multi-model mean. These results anticipate major terrestrial ecosystem changes in the Pyrenees, including significant spatiotemporal changes in hydrological resources potentially affecting millions of people living in large lowland cities.

1. Introduction

Snowfall is a relevant climatic variable in many mountain environments and affects the Earth energy balance (Thackeray et al., 2019), water resources and hydropower generation (Donnelly et al., 2017), tourism industry (François et al., 2023) or ecosystem dynamics, drought patterns, biodiversity, and agricultural timing (IPCC, 2022). Heavy snowfall events can trigger major impacts, including large-scale floods (Ionita et al., 2020), disruptions in transport systems (Faranda et al., 2022), avalanche risks (Peitzsch et al., 2021) as well as damages to forests, equipments and infrastructures (Bebi et al., 2009). A thorough understanding of spatial and temporal patterns of snowfall, including extreme events, is thus needed to maximize snowfall as a resource and mitigate its potential associated risks. Moreover, within the current warming trend, an evaluation of the future evolution of snowfall is essential for anticipating forthcoming alterations.

At hemispheric-scale, snowfall evolution projections indicate an overall reduction in the Northern Hemisphere by the mid to end of the 21st century (De Vries et al., 2014; Räisänen, 2016; IPCC, 2022). In European mountains, snowfall and snow-climate-related indicators are projected to decrease, with more significant reductions at lower elevations (López-Moreno et al., 2013; Piazza et al., 2014; Frei et al., 2018; Marty et al., 2017; IPCC, 2022; Kotlarski et al., 2023). In the Pyrenees, where this research focuses, snow is highly sensitive to warming, with reductions of 30 % per 1 °C of warming at around 1500 m (Bonsoms et al., 2023). However, predicting the future evolution of snowfall remains challenging, as winter precipitation trends are highly uncertain (López-Moreno et al., 2011) due to varying climate model projections in mid-latitude and Mediterranean regions (Peña-Angulo et al., 2020; Vicente-Serrano et al., 2022). In this context, past (ca. 1980–2010)

* Corresponding author.
E-mail address: josepbonsoms5@ub.edu (J. Bonsoms).

https://doi.org/10.1016/j.atmosres.2025.107912
Received 23 February 2024; Received in revised form 29 December 2024; Accepted 2 January 2025
Available online 3 January 2025

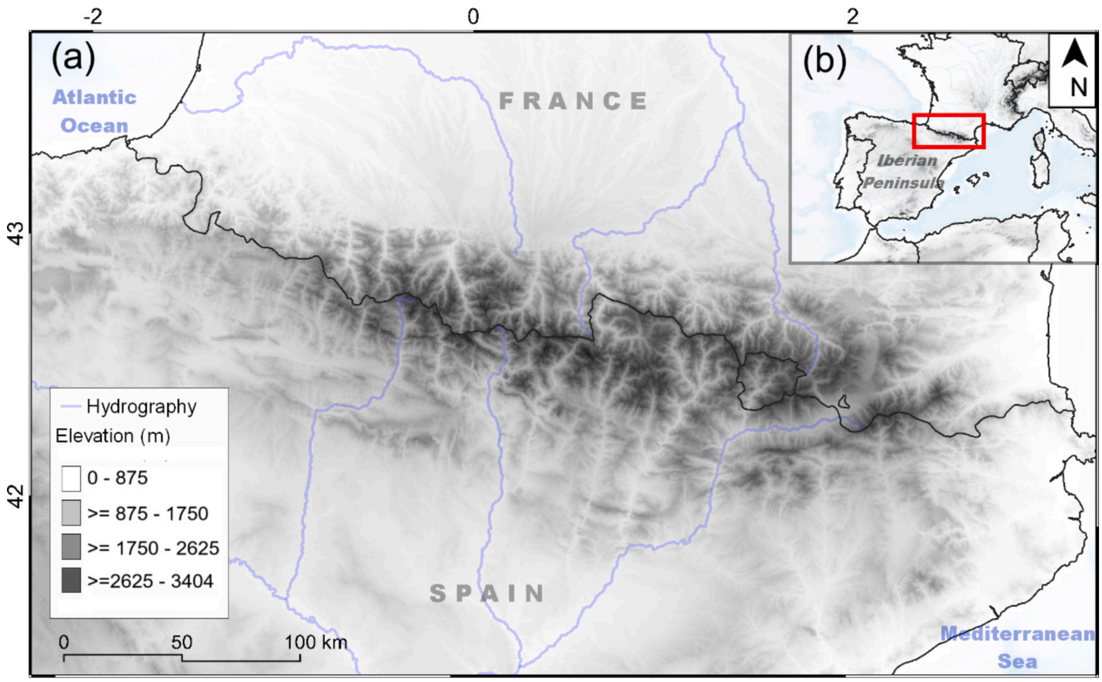

Fig. 1. Location map of the Pyrenees (a) within the Iberian Peninsula (b).

winter snow accumulation trends in the Pyrenees have exhibited significant decadal and interannual variability, governed by precipitation fluctuations. Non-statistical changes were observed in mid- and short-term periods (Bonsoms et al., 2021), while statistically significant reductions occurred over long-term periods (i.e., 1960–2015), linked to climate warming (López-Moreno et al., 2020; Bonsoms et al., 2022). For the future, although warming is expected to decrease snowfall, extreme snowfall events are not likely to diminish to the same extent (O'Gorman, 2015). Yet, extreme snowfall events are anticipated to decrease at low elevations but exhibit minimal changes and increases in cold and high-elevated sectors (Quante et al., 2021), as projected for the western United States (Lute and Abatzoglou, 2014), Italy (Derrico et al., 2022), Japan (Sasai et al., 2019), and the European Alps (Piazza et al., 2014; Le Roux et al., 2023). Extreme snowfall events in the Pyrenees are projected to decrease at low elevations (< 1500 m), but increases are expected at elevations >2000 m on central and eastern southern slopes (López-Moreno et al., 2011).

The snowfall patterns in the Pyrenees exhibit significant variability due to differences in the exposure of the massifs to air masses and elevation (López-Moreno et al., 2020; Bonsoms et al., 2022; Bonsoms et al., 2023). However, studies analyzing the future evolution of snowfall, extreme events, and return levels at high resolution remain scarce. This study aims to address this objective by analyzing data from a high-resolution (2 km) model and an ensemble of CMIP5 General Circulation Models (GCMs). The specific objectives are as follows:

a) Quantify the projected frequency and intensity of snowfall, extreme snowfall, and extreme snowfall return levels across the range.
b) Analyze spatial and temporal differences based on emission scenarios and elevation.
c) Determine uncertainties in snowfall among climate models.

2. Study area

The Pyrenees is a mountain range located in SW Europe that spans ca. 450 km between the Atlantic Ocean (West) and the Mediterranean Sea (East) (Fig. 1). The highest mountain peaks exceed 3000 m a.s.l (Aneto, 3404 m) in the central part of the range and decrease towards the margins. The prevailing climate during the winter season is influenced by the westward advection of cold jet streams, with snowfall events related with negative North Atlantic Oscillation (NAO) phases in the southern slopes of the range (López-Moreno, 2005). Precipitation is on average around 1000 mm/year although there are large spatial differences and maximum levels exceed 2500 mm/year in the northern and western slopes mountain summits (Lemus-Canovas et al., 2019). Extreme precipitation events are generally recorded during autumn in the Eastern Pyrenees (Mediterranean-climate influence) and winter and spring in the Western Pyrenees (Atlantic-climate influence) (Beguería et al., 2009). The average annual temperature is around 8 °C, with and elevation lapse rate of around 0.4 °C/100 m (Bonsoms and Ninyerola, 2023).

The snow season typically starts around November (October) and extends until the beginning of March (June) at approximately 1500 m (2500 m) (Bonsoms et al., 2022). Snow drives large runoff variability (> 40 %) of spring streamflow (López-Moreno and García-Ruiz, 2004), controls alpine plant phenology (Revuelto et al., 2022) and influences winter tourism activities (Pons et al., 2015). Indeed, with dozens of ski resorts distributed across the northern and southern slopes of the Pyrenees, snow activities play a key role in the regional socio-economic activities within the same range as well as far beyond it.

3. Data and methodology

3.1. Atmospheric model

We analyzed past and future snowfall (SF) and precipitation (P) datasets modeled using the Système d'Analyze Fournissant des Renseignements Atmosphériques à la Neige (SAFRAN atmospheric model), and available in Quintana-Seguí et al. (2022). A detailed description of SAFRAN can be found in Durand et al. (1993, 1998), with the specific version used in this work described in Quintana-Seguí et al. (2008, 2017).

SAFRAN uses an optimal interpolation algorithm to combine observational data from Spanish and French meteorological agencies (AEMET and Météo-France, respectively) with model outputs forced with ERA5, creating a gridded dataset of meteorological variables. The model

Table 1
Name and acronyms of the downscaled and bias-corrected CMIP5 GCMs included in this work.

Name	Acronym
Beijing Climate Center Climate System Model	bcc csm1
Centre National de Recherches Météorologiques Coupled Global Climate Model, version 5	CNRM-CM5
Institute of Numerical Mathematics Climate Model Version 4	INMCM4
Model for Interdisciplinary Research on Climate Institute – Earth System Model	MIROC-ESM
Max Planck Institute Earth System Model, medium resolution	MPI-ESM-MR

divides the Pyrenees into climatically homogeneous zones, typically smaller than 1000 km^2, where weather variables, particularly P, are relatively uniform. For each zone, vertical profiles of variables are estimated at 300 m intervals, and these values are interpolated spatially according to elevation. P is defined as SF when the air temperature is below 0.5 °C.

Future SF and P projections were modeled using downscaled and bias-corrected CMIP5 General Circulation Models (GCMs) (see Section 3.2). The dataset has a daily temporal resolution and a spatial resolution of 2.5 km (ETRS89 datum 30 N; EPSG: 25830). SAFRAN has been previously validated (Quintana-Seguí et al., 2022, and references therein) and implemented in France (Quintana-Seguí et al., 2008), Spain (Quintana-Seguí et al., 2017) or Tunisia (Tramblay et al., 2019), including mountain terrain such as the Pyrenees (López-Moreno et al., 2020; Vernay et al., 2022).

3.2. CMIP5 GCMs models

The future SF and P evolution is evaluated based on the downscaled CMIP5 GCMs (Table 1) bias-corrected with the analog method described at Quintana-Seguí et al. (2017). We analyzed two greenhouse gases emissions scenarios, corresponding to a medium (RCP4.5), and high (RCP8.5) greenhouse gases emission scenario. RCP4.5 estimates actual levels of CO_2 emissions until 2050 and a subsequent decrease by 2100. RCP8.5 suggest business as usual greenhouse gases emissions and an increase of CO_2 by 2075.

3.3. Indicators

We analyzed SF and extreme snowfall (SF95) accumulated snowfall for per season. We further analyzed if SF and SF95 evolution is associated with changes in frequency or related to changes in snow accumulation per event. SFdays and SF95days correspond to the number of SF and SF95 days per season, respectively. SF95 are considered when daily values exceed >95th percentile over the 1960–2006 period. Data was examined at grid scale, for winter months (December, January and February, included) between 1960 and 2100. We also analyzed the accumulated precipitation (P) to interpret if SF changes are linked to P variability in combination with the projected increase in temperature (Amblar-Francés et al., 2020).

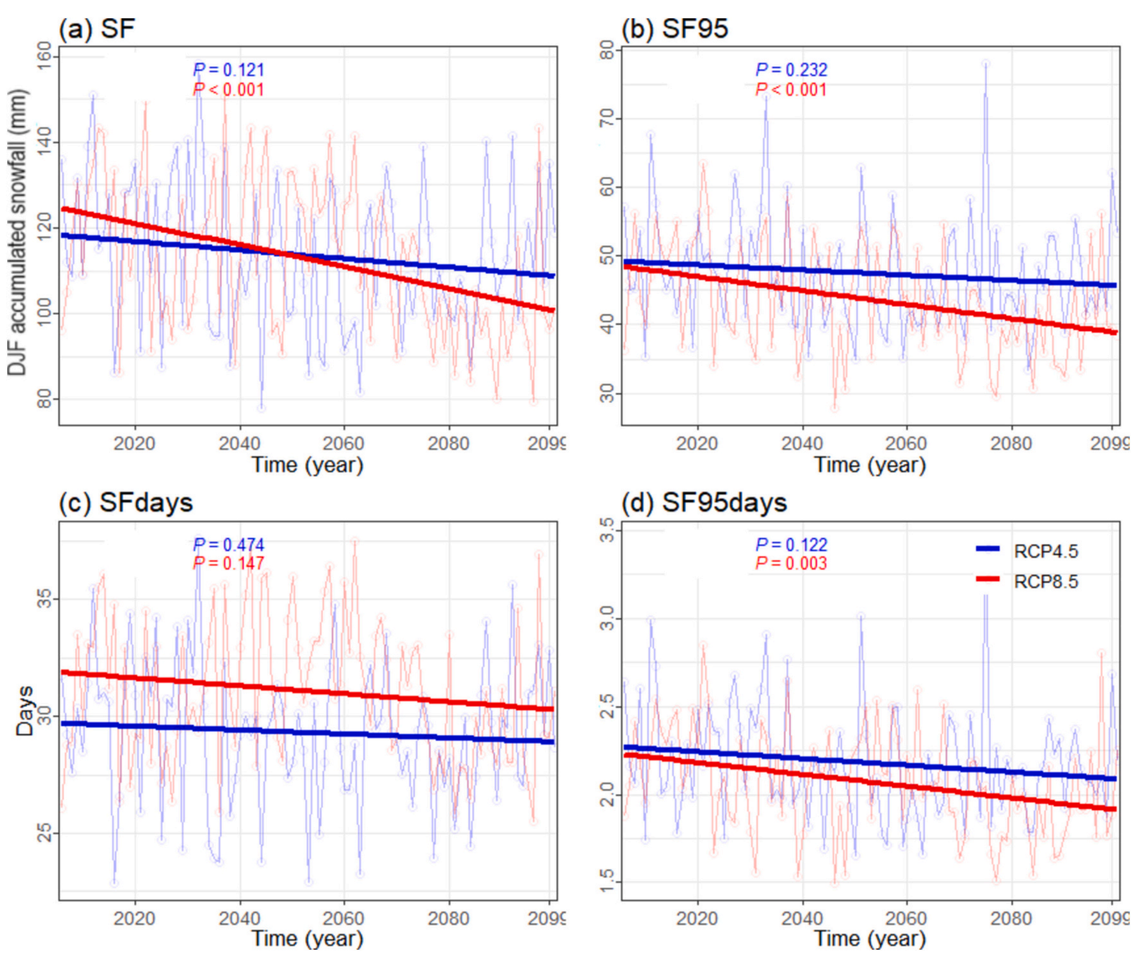

Fig. 2. Average accumulated snowfall (SF) per season (a), average accumulated extreme snowfall (Percentile ≥95th) (SF95) per season (b), average snowfall days (SFdays) per season (c) and average seasonal extreme snowfall days (SF95days) per season (d). Data are shown for RCP4.5 (blue color) and RCP8.5 (red color) scenarios. The temporal period spans from 2006 to 2100. (For interpretation of the references to color in this figure legend, the reader is referred to the web version of this article.)

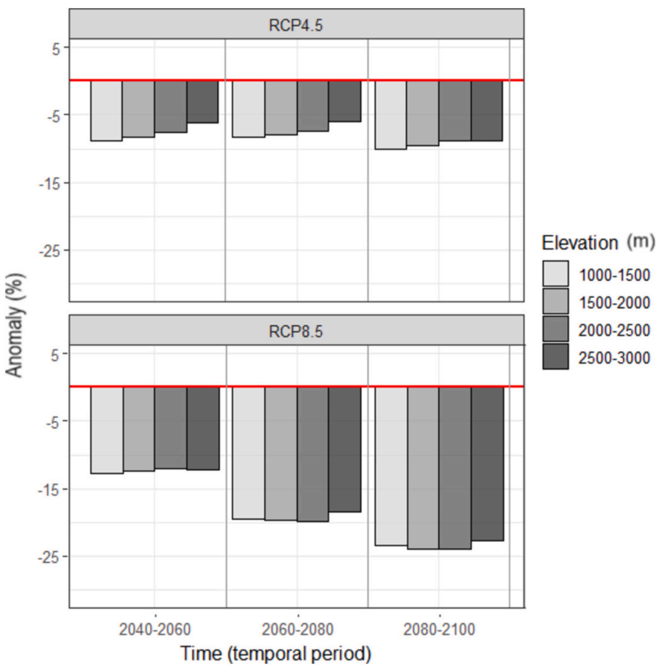

Fig. 3. Average accumulated precipitation per season (P) anomalies with respect to the historical climate period (1960–2006). Data is grouped by elevation (colors), indicator (rows) and RCP4.5 and RCP8.5 scenarios (columns). Anomalies are determined by computing the difference between future projections for different temporal periods, CMIP5 GCMs and scenarios, and their corresponding historical climate periods. The obtained data are subsequently divided by the respective historical climate periods and multiplied by 100.

3.4. Return periods (RPs) estimation

To estimate the return levels, we first calculated the maximum daily SF per year following the block maxima approach. The GEV distribution is then fitted to this set of maximum yearly values, providing a probabilistic representation of extreme SF occurrences for a given RP. Such an approach allowed us to understand the statistical properties of future extreme SF events, providing an estimation of return levels from 2 to 200-year return period (RP). The shape, scale, and location parameters of the GEV distribution play crucial roles in capturing the characteristics of extreme events. The cumulative distribution function (CDF) is the result of the Frechet, Gumbel, and Weibull families in a CDF:

$$F(x) = exp\left\{ -\left[1 + \xi\left(\frac{x-\mu}{\sigma}\right)\right]^{-1/\xi} \right\}$$

The ξ,μ and σ correspond to the shape, location and scale of the GEV distribution, respectively. These parameters were estimated by fitting the GEV distribution to the annual maxima extracted through the block maxima approach, using L-moments as the estimation method. The tail distribution depends on the ξ value, that can be as follows:

$\xi > 0$ giving the heavy-tailed Fréchet case;
$\xi = 0$ giving the light-tailed Gumbel case;
$\xi < 0$ giving the short-tailed negative-Weibull case.

The GEV distribution was fitted separately for each CMIP5 model and for each experiment (historical, RCP4.5, and RCP8.5), allowing us to account for differences in the representation of extreme SF events across models and emission scenarios.

3.5. Tendency analysis

Future snowfall evolution is analyzed by subtracting anomalies between the historical period (1960–2006) and future periods for each model, scenario, and temporal periods, corresponding to 2040–2060, 2060–2080 and 2080–2100. We also analyzed SF and SF95 frequency and intensity trends with the modified non-parametric Mann-Kendall trend test (Mann, 1955; Kendall, 1948) and the Sen's slope (Sen, 1968). To avoid false positive trends, data was detrended with the Sen's slope and the lag-1 autocorrelation coefficient (Hamed and Rao, 1998). Trends are considered statistically significant when the p-value is $\leq$0.05.

4. Results

4.1. Future winter snowfall and precipitation evolution

The future evolution of SF and SFdays indicates a negative trend across all elevation ranges (Fig. 2). Declines are particularly pronounced at elevations below 2000 m (Figs. 2 to 4). Under the RCP4.5 scenario, SF reductions are more stable over time compared to RCP8.5. During the 2040–2060 period, SF under RCP4.5 decreases on average by 28 % (1000–1500 m) to 7 % (2500–3000 m) (Fig. 4). Similarly, for the 2080–2100 period, SF reductions under RCP4.5 range from 24 % (1000–1500 m) to 9 % (2500–3000 m). In contrast, the RCP8.5 scenario exhibits a sharper decline in SF, especially after 2050 (Figs. 2 and 4). For the 2080–2100 period, SF reductions under RCP8.5 range from 29 % (1000–1500 m) to 23 % (2500–3000 m). Furthermore, trends in SF under RCP8.5 towards 2100 are statistically significant at the 0.05 level across most of the Pyrenees, while for RCP4.5, they are significant only on the southern slopes (Fig. S1).

P exhibits a negative trend under both RCP4.5 and RCP8.5 scenarios. Under RCP4.5, P decreases remain relatively constant throughout 2100, ranging from 8 % (1000–1500 m) to 6 % (2500–3000 m) (Fig. 3). Under RCP8.5, P shows largest decline after 2050. During the 2040–2060 period, P reductions under RCP8.5 range from 13 % (1000–1500 m) to 12 % (2500–3000 m). By the 2080–2100 period, P reductions under RCP8.5 reach up to 23 % across all elevation bands. The largest reductions are projected for the northern slopes, where P under RCP8.5 decreases by up to 30 % by the 2080–2100 period (Fig. 4).

4.2. Future extreme snow events

SF95 exhibits greater spatial variability than SF and P but smaller overall decreases (Fig. 4). Under RCP4.5, SF95 decreases remain relatively stable throughout the future period, with a reduction from 14 % (1000–1500 m) to 2 % (2500–3000 m). Under RCP8.5, SF95 decreases between 2040 and 2060 an average of 10 % across all elevation bands. By 2080–2100, reductions are projected to range from 18 % (1000–1500 m) to 25 % (2500–3000 m). For both scenarios, SF95 decreases across the range, with slight increases observed in the central and eastern Pyrenees (Fig. 4).

SF95 and SF95days decrease align with the results from RP levels. The evolution of maximum daily SF RPs for historical and future scenarios across different elevation bands is shown in Fig. 5. Below 2500 m, maximum daily SF RPs are projected to decrease significantly compared to the historical scenario, especially under RCP8.5. While a clear decrease in maximum daily SF RPs is expected for future scenarios, it is important to note that at 2500–3000 m, maximum daily SF RPs may still occur, similar to those in historical periods.

4.3. CMIP5 GCMs variability

There is general agreement on a long-term decrease in all indicators across CMIP5 GCMs and future scenarios for the entire mountain range (Figs. 2, S1 to S3). However, discrepancies exist in the magnitude and direction of anomalies between CMIP5 GCMs, based on elevation bands (Figs. 8 and 9) and spatial zones (Figs. S4 to S7). Differences in CMIP5 GCMs analyzed in this study are shown in Figs. 6 to 9. For SF, the largest inter-model difference is observed for the CNRM model, which presents SF anomalies of up to +20 % compared to the multi-model average at

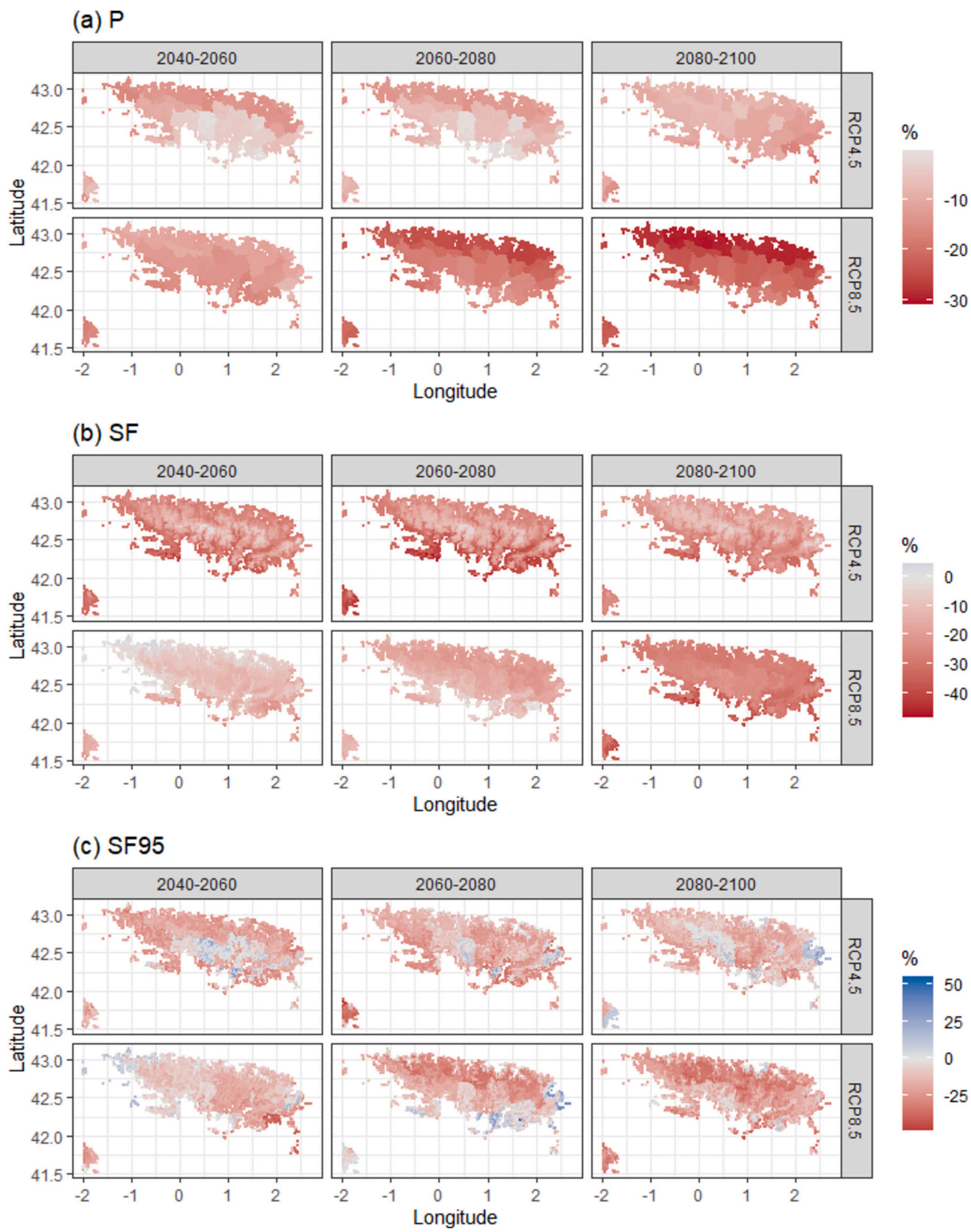

Fig. 4. Spatial anomalies with respect to the historical climate period (1960–2006) for average accumulated precipitation per season (P), average accumulated snowfall per season (SF) and average accumulated extreme snowfall (percentile >95th) (SF95) per season. Anomalies are determined by computing the difference between future projections for different temporal periods, CMIP5 GCMs, and scenarios, and their corresponding values from the historical climate period. The obtained data are subsequently divided by the respective historical climate period and multiplied by 100.

1000–1500 m under RCP4.5 (Fig. 7). In contrast, the MIROC ESM model consistently underestimates SF relative to the multi-model ensemble average, with anomalies ranging from −23 % (SF; 1000–1500 m, RCP4.5) to −4 % (SFdays; 2500–3000 m, RCP4.5) (Fig. 6). Similarly, the INMCM4 model underestimates all indicators, with SF and SFdays anomalies of −5 %, and SF95 and SF95days anomalies of +5 %. The MPI ESM-MR model tends to overestimate all indicators by +5 %, while the bcc csm1 model closely follows the multi-model average.

There is greater consensus among CMIP5 GCMs for SF than for SF95. Specifically, for SF95 under RCP4.5, the bcc csm1 and MPI ESM-MR models suggest increases at 2500–3000 m, while other CMIP5 GCMs project decreases, with variations depending on the time window (Fig. 9). For SF95 under RCP8.5, most models project decreases, but with differing magnitudes of anomalies (Fig. 9). INMCM4 and bcc csm1 show the smallest SF95 reductions, while MIROC ESM projects the largest reductions across all elevations and time periods.

5. Discussion

5.1. Past and future evolution of winter snowfall and precipitation

Results consistently anticipate reductions of SF, SFdays, SF95, and SF95days independently of the elevation range, scenario and GCM model. These results contrast with recent trends for winter snow depth

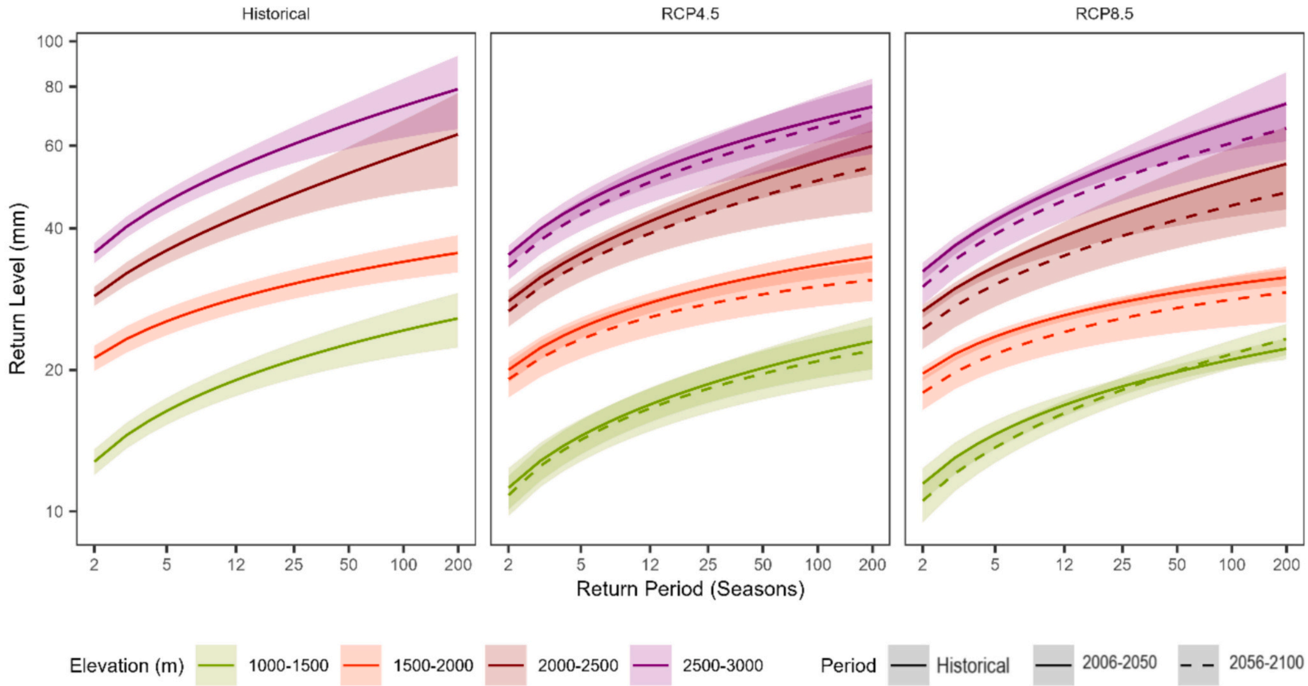

Fig. 5. Return periods of maximum daily snowfall per season. Return periods are shown for 2 to 200 years, across 4 elevation ranges, different temporal periods and for both historical and future scenarios (RCP4.5 and RCP8.5).

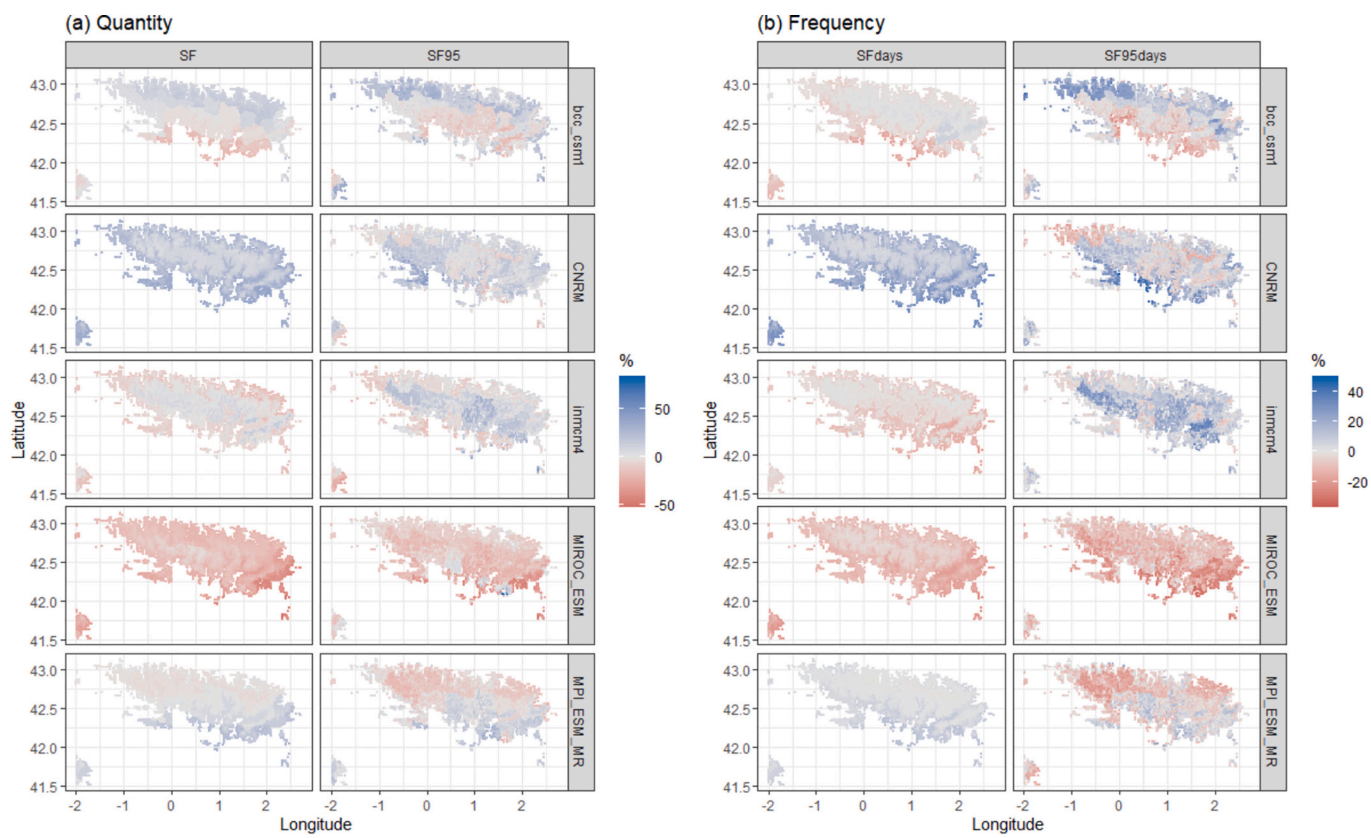

Fig. 6. Accumulated winter snowfall for a season (SF) (a) and number of winter snowfall days for a season (SFdays) (b) anomaly maps grouped by CMIP5 GCM. Anomalies are determined by computing the difference between each CMIP5 GCM and the average of the CMIP5 GCMs. The obtained data are subsequently divided by the average CMIP5 GCM and multiplied by 100.

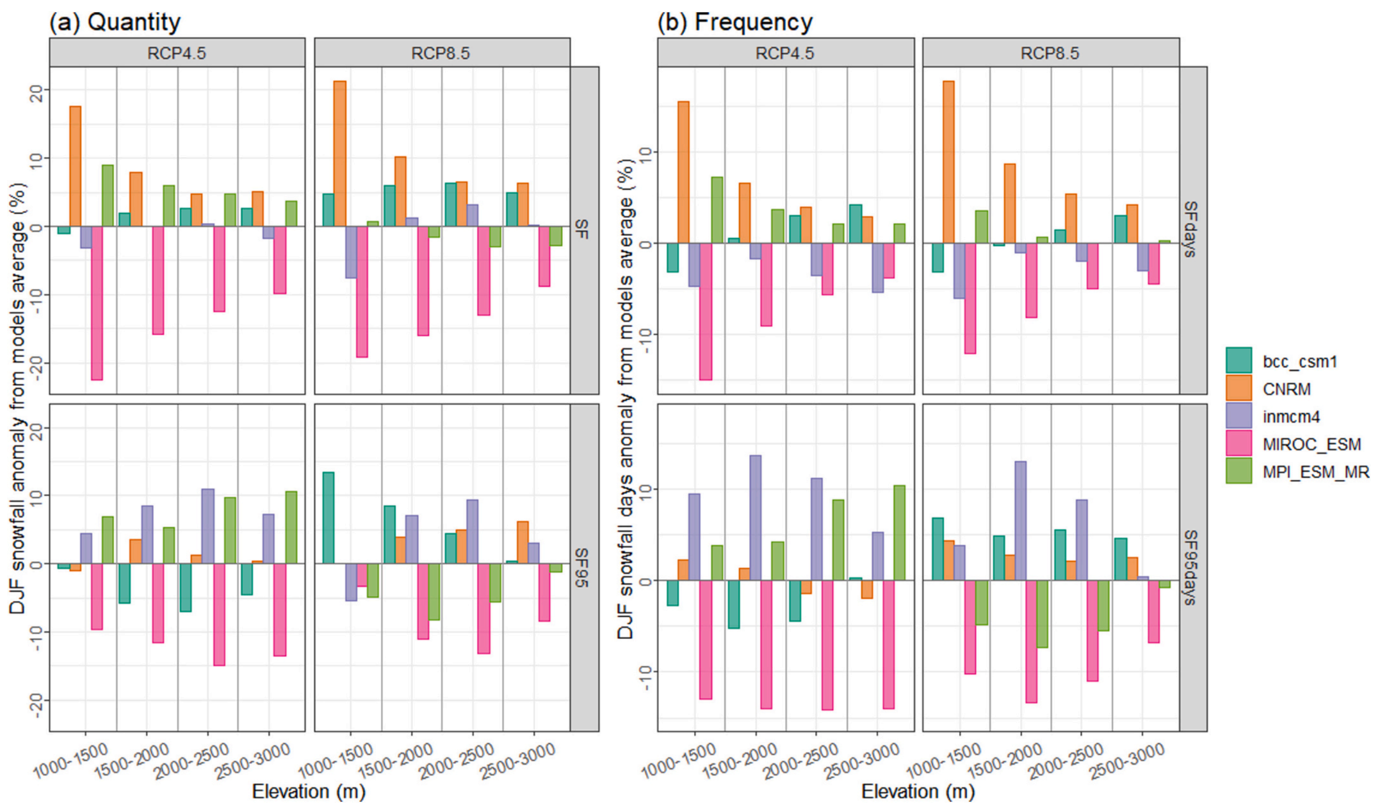

Fig. 7. Anomalies from the average values from CMIP5 GCMs for accumulated winter snowfall for a season (SF) (a) and number of winter snowfall days for a season (SFdays) (b). Data is grouped by models (colors), elevation range (x-axis), scenarios (columns) and indicators (rows). Anomalies are calculated by calculate the difference between the CMIP5 GCMs value and the CMIP5 GCM average, divided by the CMIP5 GCM average and multiplied by 100.

and snow days showing a positive tendency in the southern (ca. 1980–2010) (Buisan et al., 2015) and eastern Pyrenees (2000–2018 period) (Bonsoms et al., 2021), which was attributed to the high-decadal and interannual variability of mid-latitude precipitation as well as lower warming trends during the cold season (OPCC-CTP, 2018). Long-term (1960–2018) snow days and snow cover trends, however, indicate a negative trend associated with warming conditions in winter and early spring (López-Moreno et al., 2020).

The projected reductions in SF and SF95 in the Pyrenees align with the anticipated warming trends for the mid to late 21st century (Amblar-Francés et al., 2020). The P decreases reported in this work, up to – 23 % for RCP8.5 (2080–2100) with respect to the historical period (Fig. 3), are larger than previous results in the mountain range that projected a small (+ – 10 %) variability of winter P for both RCP4.5 and RCP8.5 (Amblar-Francés et al., 2020). Multi-model ensemble means anomalies project a decrease of SF and SF95 that is consistent with Tau MK trends (Fig. S1). Results indicate that the decrease in SF is less pronounced for RCP8.5 than for RCP4.5 until the period 2060–2070 even at lower elevations (< 2000 m) (Fig. S1). This is attributed to decreases in P RCP8.5 for 2050 onwards. Climate variability, however, is likely to result in some periods of similar than historical averages for SF95 (Fig. 4c). In addition, future extreme SF RPs at 2500–3000 m could reach similar values than historical periods (Fig. 5). The higher-than-average decrease in P observed in the northern slopes of the Pyrenees (Fig. 4a) could be attributed to the future variability of the Western Mediterranean Oscillation (WeMO), which plays a crucial role in controlling snow accumulation during winter ($r > 0.5$) in these northern slopes (Bonsoms et al., 2021). Nevertheless, additional research is necessary to comprehensively understand the interplay among atmospheric circulation patterns and their role in controlling future winter SF.

These results are in line with the projected decreases in SF across the European continent (De Vries et al., 2014; Räisänen, 2016). However, the results are not in line with increases in P anticipated for other mountain zones, such as the European Alps. Here, winter P in the NW sector has shown statistically significant increases of 20 to 40 % per century (1903–2010 period), with recent decades showing accelerated trends (Ménégoz et al., 2020). However, recent winter snow accumulation trends (ca. 1970–2020) have exhibited high interannual variability (Matiu et al., 2021). For the future, P is projected to rise for the period 2070–2099 compared to the 1981–2010 period (Rajczak and Schär, 2017). Seasonal mean P will increase by approximately +10 % (RCP4.5) to +15 % (RCP8.5) (Kotlarski et al., 2023), in contrast to the reductions of P reported in our work. The small SF and SF95 changes reported at high-elevations in the Pyrenees (i.e., −5 % at 2500–3000 m) are consistent with previous results found in the Alps, where no differences and slight increases in SF are projected in winter for high elevations (>2000 m) in both RCP4.5 and RCP8.5 scenarios towards mid-end 21st (Frei et al., 2018).

5.2. Past and future evolution of extreme events

Long-term extreme precipitation temporal trends show a general decrease in intensity and magnitude in peninsular Spain (López-Moreno et al., 2010; Serrano-Notivoli et al., 2018), except in NW Iberia, the Guadalquivir River Valley, and the Mediterranean coastal fringe (ca. 1950 to 2020 period) (Beguería et al., 2023). This contrasts with trends in other southern European mountain ranges, such as the Mediterranean-influenced southern Alps, where positive extreme P trends were found (1958–2017) (Blanchet and Creutin, 2022). Additionally, in the French Alps (1959–2019), extreme SF RPs increased by 23 % at 2000 m but decreased by 10 % at 500 m (Le Roux et al., 2021a).

Previous projections of extreme SF in the Pyrenees indicated negative trends for the 25-year return level at elevations below 1500 m and positive trends at elevations above 2500 m (López-Moreno et al., 2011).

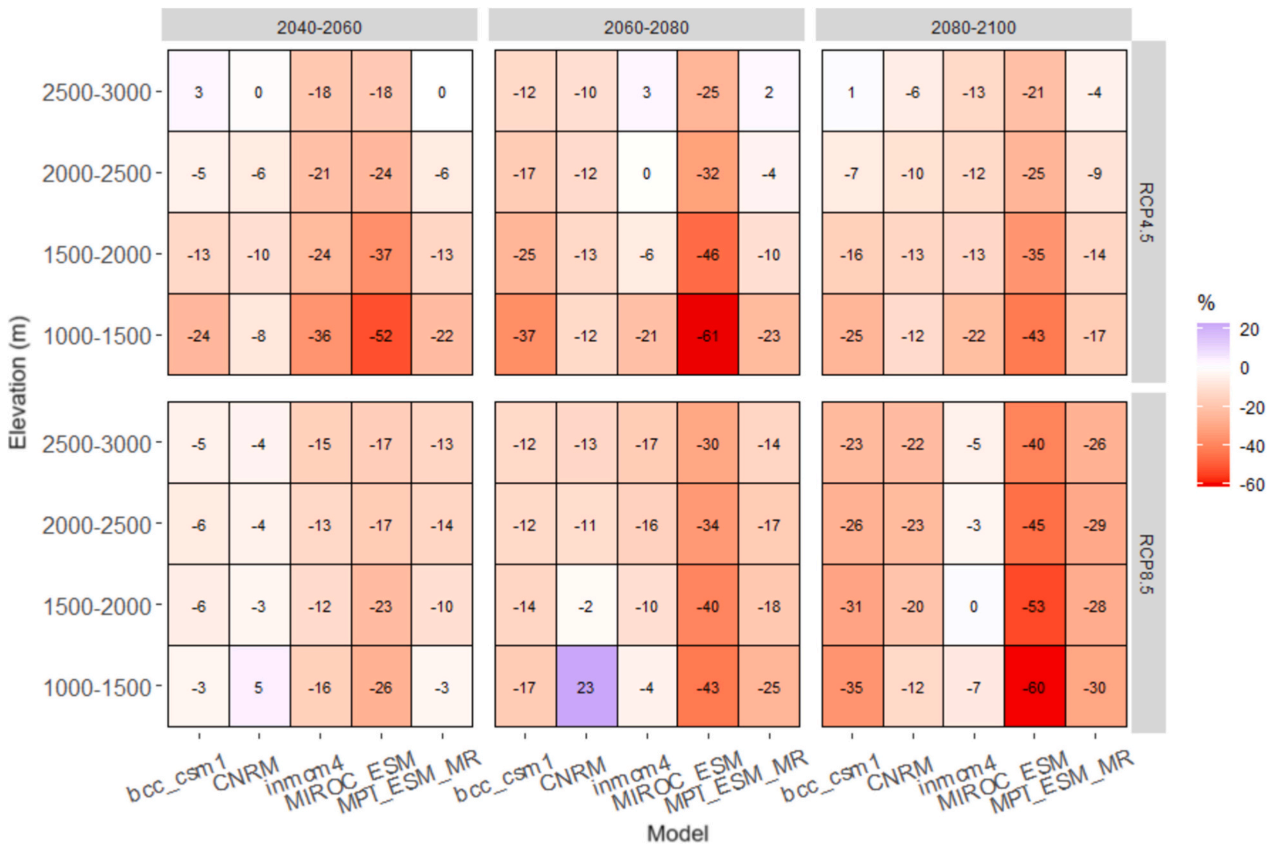

Fig. 8. Accumulated winter snowfall (SF) anomalies with respect to the historical period (1960–2006). Data is grouped by RCP4.5 (upper box) and RCP8.5 (bottom box), elevation range (y-axis) and CMIP5 GCMs (x-axis). Anomalies are determined by computing the difference between future projections for different temporal periods, models, and scenarios, and their corresponding values from the historical climate period. The obtained data are subsequently divided by the respective historical climate period and multiplied by 100.

However, our results show a general reduction in SF95 and SF95days, with only small changes observed at 2500–3000 m. Similarly, extreme SF increases have been also documented in other mountain regions, such as in Japan (Kawase et al., 2016) and the Alps (Le Roux et al., 2021b). The increase of extreme SF RPs projected to high elevated alpine regions (Piazza et al., 2014; Frei et al., 2018; Le Roux et al., 2023), was attributed to greater atmospheric moisture-holding capacity within a warmer climate, which is estimated to result in approximately a 7 % increase in precipitation per °C (O'Gorman, 2015). In the Mediterranean region, increases in extreme SF events was attributed to higher temperatures, more moisture availability, convective events, and more favorable synoptic conditions for extreme events (Derrico et al., 2022; Faranda, 2020).

5.3. Snowfall and precipitation projection uncertainties

We analyzed a high-resolution downscaled (2.5 km) dataset, which reduces uncertainties associated with GCMs in mountainous regions due to their complex topography (Mudryk et al., 2020). The SAFRAN model integrates meteorological data and in-situ observations through an optimal interpolation algorithm (Quintana-Seguí et al., 2017). Its performance has been evaluated against Météo-France's observational network, yielding root-mean-square errors of 1.5 °C for temperature and 2.4 mm/day for precipitation (Quintana-Seguí et al., 2008). These discrepancies are attributed to the spatial heterogeneity of precipitation within large analysis zones (1000 km^2), the limited representativity of the observational stations used for validation, the interpolation scheme's inability to fully capture the annual temperature cycle, and the model's limitations in accurately reproducing extreme precipitation events (Quintana-Seguí et al., 2008, 2017). In mountainous regions, additional uncertainties arise from the sparse availability of climate records and changes in the locations of meteorological stations (Vernay et al., 2022). SAFRAN is operated by Météo-France for diverse applications and is frequently coupled with other land-surface models (e.g., Quintana-Seguí et al., 2017; Vernay et al., 2022). The model has been validated and implemented in various geographical contexts, including continental France (Quintana-Seguí et al., 2008), Spain (Quintana-Seguí et al., 2017), and Tunisia (Tramblay et al., 2019). SAFRAN has been employed to analyze long-term trends in snow depth and cover (López-Moreno et al., 2020), extreme snowfall events (Le Roux et al., 2021a), and future snow projections in the Alps (Verfaillie et al., 2018), demonstrating reliability in these applications. The gridded version of SAFRAN utilized in the present study (Quintana-Seguí et al., 2022) has been validated and applied in the study area for evapotranspiration modeling (Dari et al., 2022), assessments of long-term flood trends (Llasat et al., 2024), and hydrological modeling, including validations against in-situ records (Clavera-Gispert et al., 2023).

There is general agreement on a reduction in SF and SF95. However, the CMIP5 GCMs analyzed here show differences inf SF projections, with anomalies up to +20 % over the multi-model ensemble (Fig. 7). This highlights the challenges in accurately projecting future SF and SF95 in the mountain range. In addition, some CMIP5 GCMs project stable or increasing SF95 under RCP4.5, while others projected the opposite (Figs. 8 and 9), emphasizing the importance of analyzing multiple GCMs. These differences among GCMs suggest uncertainties in snowpack projections based on single GCMs and multi-model ensembles, with direct implications for future water resource assessments and their related impacts.

The high interannual variability of SF aligns with projections for mid-latitude winter P (Coppola et al., 2021) a factor strongly influencing

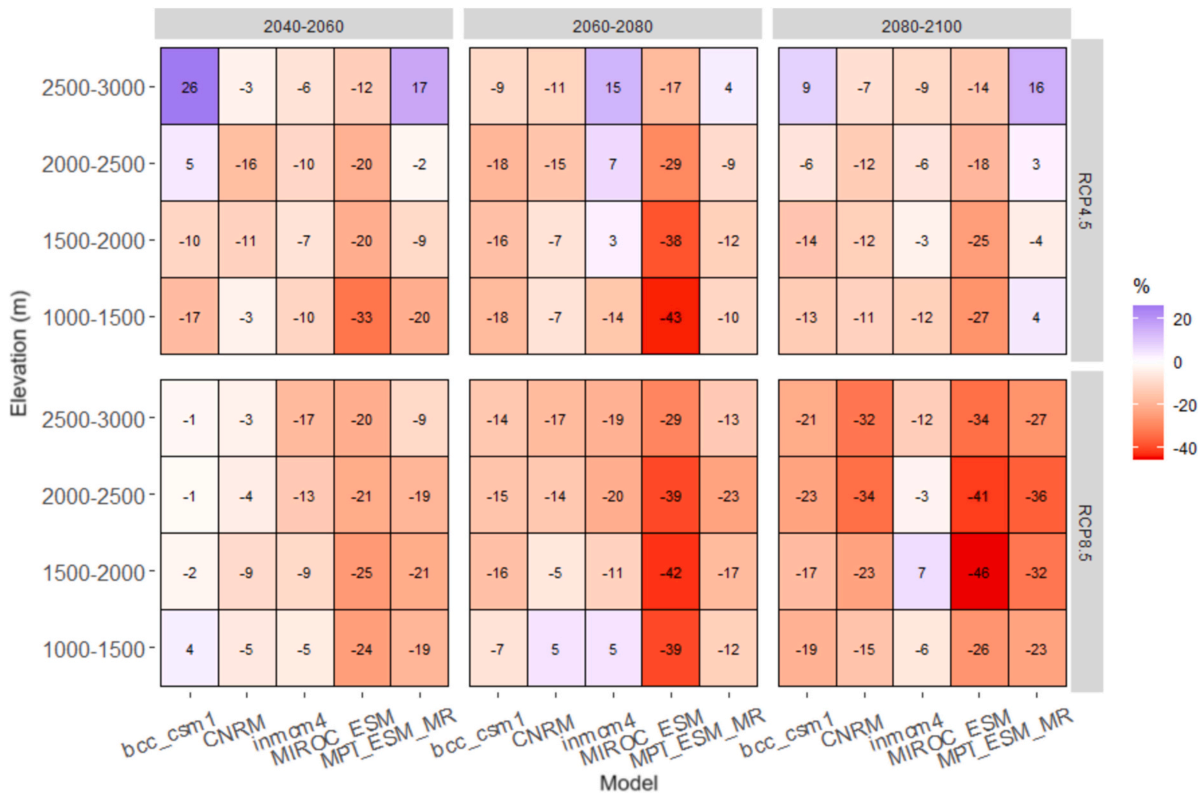

Fig. 9. Accumulated winter extreme snowfall (SF95) anomalies with respect to the historical period (1960–2006). Data is grouped by RCP4.5 (upper box) and RCP8.5 (bottom box), elevation range (y-axis) and CMIP5 GCMs (x-axis). Anomalies are determined by computing the difference between future projections for different temporal periods, models, and scenarios, and their corresponding values from the historical climate period. The obtained data are subsequently divided by the respective historical climate period and multiplied by 100.

hydroclimate trends in southwestern Europe (Hannaford et al., 2013; Peña-Angulo et al., 2020). Differences in mid-latitude precipitation among climate models have been linked to the influence of mid-latitude annular modes of internal variability (Deser et al., 2012). CMIP5 and CMIP6 models have shown biases in spatial patterns and precipitation magnitudes (Vicente-Serrano et al., 2022). Comparisons of winter precipitation in southwestern Europe, using in-situ records, reanalysis data, and climate model projections (CMIP3, CMIP5, and CMIP6), reveal discrepancies between observed and modeled precipitation, which also extend to trends (Peña-Angulo et al., 2020). This work analyzed CMIP5 projections, and future works should compare the results presented here with CMIP6 bias-corrected and downscaled projections to assess potential differences.

6. Conclusions

We conducted an analysis of future SF and SF95 patterns in the Pyrenees using a multi-model approach with CMIP5 GCMs and two greenhouse gas concentration pathways. Data consistently indicates an overall reduction in SF, SF95, SFdays and SF95days. The results reveal non-linear declines in all indicators, with more pronounced losses at lower elevation sectors. Specifically, projections for the end of the 21st century (2080–2100 period) under SF RCP4.5 anticipate reductions ranging from −24 % (1000–1500 m) to −9 % (2500–3000 m), while SF RCP8.5 ranges from −29 % (1000–1500 m) to −23 % (2500–3000 m). Statistically significant decreases at the 0.05 significance level are observed for most of the mountain range under SF RCP8.5.

The long-term evolution is attributed to warming and precipitation decreases, with maximum P reductions (2080–2100 period) under RCP8.5, reaching – 30 % on the northern slopes of the Pyrenees. SF95 exhibits a negative evolution, with SF95 RCP4.5 at 1000–1500 m decreasing by −12 % (2080–2100 period) compared to the historical period. However, at 2500–3000 m, SF95 RCP4.5 multi-model averages show small (2 %) increases for the same temporal period. SF95 RCP8.5, on the other hand, indicates larger decreases of −18 % (1000–1500 m) and – 25 % (2500–3000 m) during the 2080–2100 period. Extreme SF RPs also show decreases across all scenarios and most of the elevation ranges considered. Significant inter-model differences are observed in terms of magnitude across all indicators, with certain CMIP5 GCMs overestimating (CNRM) or underestimating (MIROC ESM) inter-model averages. The disparities among these models lead to varying trends in magnitude depending on the elevation band. This variability introduces uncertainties in projecting the evolution of the snowpack based on snowfall climate projections. The study offers insights into future snowfall patterns in the Pyrenees, indicating a reduction in available hydrological resources with significant implications for mountain ecosystems and nearby cities reliant on water availability.

CRediT authorship contribution statement

Josep Bonsoms: Conceptualization, Methodology, Software, Data curation, Investigation, Formal analysis, Writing – original draft, Writing – review & editing. **Juan I. López-Moreno:** Conceptualization, Funding acquisition, Project administration, Supervision. **Marc Lemus-Cánovas:** Formal analysis, Project administration, Supervision, Writing – review & editing. **Marc Oliva:** Funding acquisition, Project administration, Supervision.

Declaration of competing interest

The authors declare no competing interests.

Data availability

The data sources are detailed in the articl

Acknowledgements

This work frames within the research topics examined by the research group "Antarctic, Artic, Alpine Environments-ANTALP" (2017-SGR-1102) founded by the Government of Catalonia, HIDROIBERNIEVE (CGL2017-82216-R) and MARGISNOW (PID2021-124220OB-100), from the Spanish Ministry of Science, Innovation and Universities. JB is supported by a pre–doctoral University Professor FPI grant (PRE2021-097046) funded by the Spanish Ministry of Science, Innovation and Universities. M.L.-C. is supported by a postdoctoral contract from the programme named "Programa de axudas de apoio á etapa inicial de formacion posdoutoral (2022)" funded by Xunta de Galicia (Government of Galicia, Spain).

Appendix A. Supplementary data

Supplementary data to this article can be found online at https://doi.org/10.1016/j.atmosres.2025.107912.

References

Amblar-Francés, M.P., Ramos-Calzado, P., Sanchis-Lladó, J., Hernanz-Lázaro, A., Peral-García, M.C., Navascués, B., Dominguez-Alonso, M., Pastor-Saavedra, M.A., Rodríguez-Camino, E., 2020. High resolution climate change projections for the Pyrenees region. Adv. Sci. Res. 191–208. https://doi.org/10.5194/asr-17-191-2020.

Bebi, P., Kulakowski, D., Rixen, C., 2009. Snow avalanche disturbances in forest ecosystems-state of research and implications for management. For. Ecol. Manag. 257, 1883–1892. https://doi.org/10.1016/j.foreco.2009.01.050.

Beguería, S., Vicente-Serrano, S.M., López-Moreno, J.I., García-Ruiz, J.M., 2009. Annual and seasonal mapping of peak intensity, magnitude and duration of extreme precipitation events across a climatic gradient, Northeast Spain. Int. J. Climatol. 29, 1759–1779. https://doi.org/10.1002/joc.1808.

Beguería, S., Tomas-Burguera, M., Serrano-Notivoli, R., Barriopedro, D., Vicente-Serrano, S.M., 2023. Evolution of Extreme Precipitation in Spain: Contribution of Atmospheric Dynamics and Long-Term Trends.

Blanchet, J., Creutin, J.D., 2022. Instrumental agreement and retrospective analysis of trends in precipitation extremes in the French Mediterranean Region. Environ. Res. Lett. 17. https://doi.org/10.1088/1748-9326/ac7734.

Bonsoms, J., Ninyerola, M., 2023. Comparison of linear, generalized additive models and machine learning algorithms for spatial climate interpolation. Theor. Appl. Climatol. https://doi.org/10.1007/s00704-023-04725-5.

Bonsoms, J., Gonzalez, S., Prohom, M., Esteban, P., Salvador-Franch, F., López-Moreno, J.I., Oliva, M., 2021. Spatio-temporal patterns of snow in the Catalan Pyrenees (NE Iberia). Int. J. Climatol. 41, 5676–5697. https://doi.org/10.1002/joc.7147.

Bonsoms, J., López-Moreno, J.I., González, S., Oliva, M., 2022. Increase of the energy available for snow ablation in the Pyrenees (1959–2020) and its relation to atmospheric circulation. Atmos. Res. 275. https://doi.org/10.1016/j.atmosres.2022.106228.

Bonsoms, J., López-Moreno, J.I., Alonso-González, E., 2023. Snow sensitivity to temperature and precipitation change during compound cold–hot and wet–dry seasons in the Pyrenees. Cryosphere 17, 1307–1326. https://doi.org/10.5194/tc-17-1307-2023.

Buisan, S.T., Saz, M.A., López-Moreno, J.I., 2015. Spatial and temporal variability of winter snow and precipitation days in the western and central Spanish Pyrenees. Int. J. Climatol. 35, 259–274. https://doi.org/10.1002/joc.3978.

Clavera-Gispert, R., Quintana-Seguí, P., Palazón, L., Zabaleta, A., Cenobio, O., Barella-Ortiz, A., Beguería, S., 2023. Streamflow trends of the Pyrenees using observations and multi-model approach (1980–2013). J. Hydrol. Reg. Stud. 46, 101322. https://doi.org/10.1016/J.EJRH.2023.101322.

Coppola, E., Nogherotto, R., Ciarlo, J.M., Giorgi, F., van Meijgaard, E., Kadygrov, N., Iles, C., Corre, L., Sandstad, M., Somot, S., Nabat, P., Vautard, R., Levavasseur, G., Schwingshackl, C., Sillmann, J., Kjellström, E., Nikulin, G., Aalbers, E., Lenderink, G., Christensen, O.B., Boberg, F., Sørland, S.L., Demory, M.E., Bülow, K., Teichmann, C., Warrach-Sagi, K., Wulfmeyer, V., 2021. Assessment of the European climate projections as simulated by the large EURO-CORDEX regional and global climate model ensemble. J. Geophys. Res. Atmos. 126. https://doi.org/10.1029/2019JD032356.

Dari, J., Quintana-Seguí, P., Morbidelli, R., Saltalippi, C., Flammini, A., Giugliarelli, E., Escorihuela, M.J., Stefan, V., Brocca, L., 2022. Irrigation estimates from space: implementation of different approaches to model the evapotranspiration contribution within a soil-moisture-based inversion algorithm. Agric. Water Manag. 265, 107537. https://doi.org/10.1016/j.agwat.2022.107537.

De Vries, H., Lenderink, G., Van Meijgaard, E., 2014. Future snowfall in western and Central Europe projected with a high-resolution regional climate model ensemble. Geophys. Res. Lett. 41, 4294–4299. https://doi.org/10.1002/2014GL059724.

Derrico, M., Pons, F., Yiou, P., Tao, S., Nardini, C., Lunkeit, F., Faranda, D., 2022. Present and future synoptic circulation patterns associated with cold and snowy spells over Italy. Earth Syst. Dynam. 13, 961–992. https://doi.org/10.5194/esd-13-961-2022.

Deser, C., Phillips, A., Bourdette, V., Teng, H., 2012. Uncertainty in climate change projections: the role of internal variability. Clim. Dyn. 38, 527–546. https://doi.org/10.1007/s00382-010-0977-x.

Donnelly, C., Greuell, W., Andersson, J., Gerten, D., Pisacane, G., Roudier, P., Ludwig, F., 2017. Impacts of climate change on European hydrology at 1.5, 2 and 3 degrees mean global warming above preindustrial level. Clim. Chang. 143, 13–26. https://doi.org/10.1007/s10584-017-1971-7.

François, H., Samacoïts, R., Bird, D.N., Köberl, J., Prettenthaler, F., Morin, S., 2023. Climate change exacerbates snow-water-energy challenges for European ski tourism. Nat. Clim. Chang. 13, 935–942. https://doi.org/10.1038/s41558-023-01759-5.

Frei, P., Kotlarski, S., Liniger, M.A., Schär, C., 2018. Future snowfall in the Alps: projections based on the EURO-CORDEX regional climate models. Cryosphere 12, 1–24. https://doi.org/10.5194/tc-12-1-2018.

Hamed, K.H., Rao, A., 1998. R.: hydrology a modified Mann-Kendall trend test for autocorrelated data. J. Hydrol. 196.

Hannaford, J., Buys, G., Stahl, K., Tallaksen, L.M., 2013. The influence of decadal-scale variability on trends in long European streamflow records. Hydrol. Earth Syst. Sci. 17, 2717–2733. https://doi.org/10.5194/hess-17-2717-2013.

Ionita, M., Nagavciuc, V., Guan, B., 2020. Rivers in the Sky, Flooding on the Ground: The Role of Atmospheric Rivers for the Inland Flooding in Central Europe.

IPCC, 2022. High mountain areas. In: The Ocean and Cryosphere in a Changing Climate. Cambridge University Press, pp. 131–202. https://doi.org/10.1017/9781009157964.004.

Kotlarski, S., Gobiet, A., Morin, S., Olefs, M., Rajczak, J., Samacoïts, R., 2023. 21st century alpine climate change. Clim. Dyn. 60, 65–86. https://doi.org/10.1007/s00382-022-06303-3.

Le Roux, E., Evin, G., Eckert, N., Blanchet, J., Morin, S., 2021a. Elevation-dependent trends in extreme snowfall in the French Alps from 1959 to 2019. Cryosphere 15, 4335–4356. https://doi.org/10.5194/tc-15-4335-2021.

Le Roux, E., Evin, G., Eckert, N., Blanchet, J., Morin, S., 2021b. Elevation-dependent trends in extreme snowfall in the French Alps from 1959 to 2019. Cryosphere 15, 4335–4356. https://doi.org/10.5194/tc-15-4335-2021.

Le Roux, E., Evin, G., Samacoïts, R., Eckert, N., Blanchet, J., Morin, S., 2023. Projection of snowfall extremes in the French Alps as a function of elevation and global warming level. Cryosphere 17, 4691–4704. https://doi.org/10.5194/tc-17-4691-2023.

Lemus-Canovas, M., Lopez-Bustins, J.A., Trapero, L., Martin-Vide, J., 2019. Combining circulation weather types and daily precipitation modelling to derive climatic precipitation regions in the Pyrenees. Atmos. Res. 220, 181–193. https://doi.org/10.1016/j.atmosres.2019.01.018.

Llasat, M.C., Llasat-Botija, M., Pardo, E., Marcos-Matamoros, R., Lemus-Canovas, M., 2024. Floods in the Pyrenees: a global view through a regional database. Nat. Hazards Earth Syst. Sci. 24, 3423–3443. https://doi.org/10.5194/nhess-24-3423-2024.

López-Moreno, J.I., 2005. Recent variations of snowpack depth in the central Spanish Pyrenees. Arct. Antarct. Alp. Res. 37, 253–260. https://doi.org/10.1657/1523-0430(2005)037[0253:RVOSDI]2.0.CO;2.

López-Moreno, J.I., García-Ruiz, J.M., 2004. Influence of Snow Accumulation and Snowmelt on Streamflow in the Central Spanish Pyrenees.

López-Moreno, J.I., Vicente-Serrano, S.M., Angulo-Martínez, M., Beguería, S., Kenawy, A., 2010. Trends in daily precipitation on the northeastern Iberian Peninsula, 1955-2006. Int. J. Climatol. 30, 1026–1041. https://doi.org/10.1002/joc.1945.

López-Moreno, J.I., Goyette, S., Vicente-Serrano, S.M., Beniston, M., 2011. Effects of climate change on the intensity and frequency of heavy snowfall events in the Pyrenees. Clim. Chang. 105, 489–508. https://doi.org/10.1007/s10584-010-9889-3.

López-Moreno, J.I., Pomeroy, J.W., Revuelto, J., Vicente-Serrano, S.M., 2013. Response of snow processes to climate change: spatial variability in a small basin in the Spanish Pyrenees. Hydrol. Process. 27, 2637–2650. https://doi.org/10.1002/hyp.9408.

López-Moreno, J.I., Soubeyroux, J.M., Gascoin, S., Alonso-Gonzalez, E., Durán-Gómez, N., Lafaysse, M., Vernay, M., Carmagnola, C., Morin, S., 2020. Long-term trends (1958–2017) in snow cover duration and depth in the Pyrenees. Int. J. Climatol. 40, 6122–6136. https://doi.org/10.1002/joc.6571.

Lute, A.C., Abatzoglou, J.T., 2014. Role of extreme snowfall events in interannual variability of snowfall accumulation in the western United States. Water Resour. Res. 50 (4), 2874–2888. https://doi.org/10.1002/2013WR014465.

Mann, H.B., 1955. Nonparametric tests against trend. Econometrica 13, 245–259.

Marty, C., Schlögl, S., Bavay, M., Lehning, M., 2017. How much can we save? Impact of different emission scenarios on future snow cover in the Alps. Cryosphere 11, 517–529. https://doi.org/10.5194/tc-11-517-2017.

Mudryk, L., Santolaria-Otín, M., Krinner, G., Ménégoz, M., Derksen, C., Brutel-Vuilmet, C., Brady, M., Essery, R., 2020. Historical Northern Hemisphere snow cover trends and projected changes in the CMIP6 multi-model ensemble. Cryosphere 14, 2495–2514. https://doi.org/10.5194/tc-14-2495-2020.

O'Gorman, P.A., 2015. Precipitation Extremes Under Climate Change. https://doi.org/10.1007/s40641-015-0009-3, 1 June.

Peitzsch, E.H., Pederson, G.T., Birkeland, K.W., Hendrikx, J., Fagre, D., 2021. B.: climate drivers of large magnitude snow avalanche years in the U.S. northern Rocky Mountains. Sci. Rep. 11. https://doi.org/10.1038/s41598-021-89547-z.

Peña-Angulo, D., Vicente-Serrano, S.M., Domínguez-Castro, F., Murphy, C., Reig, F., Tramblay, Y., Trigo, R.M., Luna, M.Y., Turco, M., Noguera, I., Aznárez-Balta, M., García-Herrera, R., Tomas-Burguera, M., El Kenawy, A., 2020. Long-term precipitation in Southwestern Europe reveals no clear trend attributable to anthropogenic forcing. Environ. Res. Lett. 15. https://doi.org/10.1088/1748-9326/ab9c4f.

Piazza, M., Boé, J., Terray, L., Pagé, C., Sanchez-Gomez, E., Déqué, M., 2014. Projected 21st century snowfall changes over the French Alps and related uncertainties. Clim. Chang. 122, 583–594. https://doi.org/10.1007/s10584-013-1017-8.

Pons, M., López-Moreno, J.I., Rosas-Casals, M., Jover, 2015. The vulnerability of Pyrenean ski resorts to climate-induced changes in the snowpack. Clim. Chang. 131, 591–605. https://doi.org/10.1007/s10584-015-1400-8.

Quante, L., Willner, S.N., Middelanis, R., et al., 2021. Regions of intensification of extreme snowfall under future warming. Sci Rep 11, 16621. https://doi.org/10.1038/s41598-021-95979-4.

Quintana-Seguí, P., Le Moigne, P., Durand, Y., Martin, E., Habets, F., Baillon, M., Canellas, C., Franchisteguy, L., Morel, S., 2008. Analysis of near-surface atmospheric variables: validation of the SAFRAN analysis over France. J. Appl. Meteorol. Climatol. 47, 92–107. https://doi.org/10.1175/2007JAMC1636.1.

Quintana-Seguí, P., Turco, M., Herrera, S., Miguez-Macho, G., 2017. Validation of a new SAFRAN-based gridded precipitation product for Spain and comparisons to Spain02 and ERA-Interim. Hydrol. Earth Syst. Sci. 21, 2187–2201. https://doi.org/10.5194/hess-21-2187-2017.

Quintana-Seguí, P., Vidal, J.-P., Le Cointe, P., 2022. PIRAGUA_Atmos_Climate [Dataset]; Observatori de l'Ebre (URL – CSIC). http://digital.csic.es/handle/10261/271116;. https://doi.org/10.20350/digitalCSIC/14666.

Räisänen, J., 2016. Twenty-first century changes in snowfall climate in Northern Europe in ENSEMBLES regional climate models. Clim. Dyn. 46, 339–353. https://doi.org/10.1007/s00382-015-2587-0.

Räisänen, J., 2016. Twenty-first century changes in snowfall climate in Northern Europe in ENSEMBLES regional climate models. Climate dynamics 46, 339–353.

Rajczak, J., Schär, C., 2017. Projections of future precipitation extremes over Europe: a multimodel assessment of climate simulations. J. Geophys. Res. Atmos. 122, 10773–10800. https://doi.org/10.1002/2017JD027176.

Revuelto, J., Gómez, D., Alonso-González, E., Vidaller, I., Rojas-Heredia, F., Deschamps-Berger, C., García-Jiménez, J., Rodríguez-López, G., Sobrino, J., Montorio, R., Perez-Cabello, F., López-Moreno, J.I., 2022. Intermediate snowpack melt-out dates guarantee the highest seasonal grasslands greening in the Pyrenees. Sci. Rep. 12. https://doi.org/10.1038/s41598-022-22391-x.

Sasai, T., Kawase, H., Kanno, Y., Yamaguchi, J., Sugimoto, S., Yamazaki, T., Iwasaki, T., 2019. Future projection of extreme heavy snowfall events with a 5-km large ensemble regional climate simulation. J. Geophys. Res. Atmos. 124 (24), 13975–13990.

Sen, P.K., 1968. Estimates of the regression coefficient based on Kendall's tau. J. Am. Stat. Assoc. 63 (324), 1379–1389.

Serrano-Notivoli, R., Beguería, S., Saz, M.Á., de Luis, M., 2018. Recent trends reveal decreasing intensity of daily precipitation in Spain. Int. J. Climatol. 38, 4211–4224. https://doi.org/10.1002/joc.5562.

Thackeray, C.W., Derksen, C., Fletcher, C.G., Hall, A., 2019. Snow and Climate: Feedbacks, Drivers, and Indices of Change. https://doi.org/10.1007/s40641-019-00143-w.

Tramblay, Y., Feki, H., Quintana-Seguí, P., Guijarro, J.A., 2019. The SAFRAN daily gridded precipitation product in Tunisia (1979–2015). Int. J. Climatol. 39, 5830–5838. https://doi.org/10.1002/joc.6181.

Verfaillie, D., Lafaysse, M., Déqué, M., Eckert, N., Lejeune, Y., Morin, S., 2018. Multi-component ensembles of future meteorological and natural snow conditions for 1500 m altitude in the Chartreuse mountain range, Northern French Alps. Cryosphere 12, 1249–1271. https://doi.org/10.5194/tc-12-1249-2018.

Vernay, M., Lafaysse, M., Monteiro, D., Hagenmuller, P., Nheili, R., Samacoïts, R., Verfaillie, D., Morin, S., 2022. The S2M meteorological and snow cover reanalysis over the French mountainous areas: description and evaluation (1958-2021). Earth Syst. Sci. Data 14, 1707–1733. https://doi.org/10.5194/essd-14-1707-2022.

Vicente-Serrano, S.M., García-Herrera, R., Peña-Angulo, D., Tomas-Burguera, M., Domínguez-Castro, F., Noguera, I., Calvo, N., Murphy, C., Nieto, R., Gimeno, L., Gutierrez, J.M., Azorin-Molina, C., El Kenawy, A., 2022. Do CMIP models capture long-term observed annual precipitation trends? Clim. Dyn. 58, 2825–2842. https://doi.org/10.1007/s00382-021-06034-x.

Durand, Y., Giraud, G., Mérindol, L., 1998. Short-term numerical avalanche forecast used operationally at Météo-France over the Alps and Pyrenees. Annals of Glaciology 26, 357–366.

Faranda, D., Bourdin, S., Ginesta, M., Krouma, M., Noyelle, R., Pons, F., Yiou, P., Messori, G., 2022. A climate-change attribution retrospective of some impactful weather extremes of 2021. Weather Clim. Dynam. 3, 1311–1340. https://doi.org/10.5194/wcd-3-1311-2022.

Durand, Y., Brun, E., Mérindol, L., Guyomarc'h, G., Lesaffre, B., et al., 1993. A meteorological estimation of relevant parameters for snow models. Ann. Glaciol. 18, 65–71.

Kawase, H., Murata, A., Mizuta, R., et al., 2016. Enhancement of heavy daily snowfall in central Japan due to global warming as projected by large ensemble of regional climate simulations. Climatic Change 139, 265–278. https://doi.org/10.1007/s10584-016-1781-3.

Kendall, M.G., 1948. Rank correlation methods.

OPCC-CTP, 2018. Climate Change in the Pyrenees: Impacts, Vulnerabilities and Adaptation Bases of Knowledge for the Future Climate Change Adaptation Strategy in the Pyrenees, 147 pp. Jaca, Spain. /editor/opcc-informe-en-paginas.pdf (last access: 30 December 2024). https://www.opccctp.org/sites/default/files.

Ménégoz, M., Valla, E., Jourdain, N.C., Blanchet, J., Beaumet, J., Wilhelm, B., Gallée, H., Fettweis, X., Morin, S., Anquetin, S., 2020. Contrasting seasonal changes in total and intense precipitation in the European Alps from 1903 to 2010. Hydrol. Earth Syst. Sci. 24, 5355–5377. https://doi.org/10.5194/hess-24-5355-2020.

Matiu, M., Crespi, A., Bertoldi, G., Carmagnola, C.M., Marty, C., Morin, S., Schöner, W., Cat Berro, D., Chiogna, G., De Gregorio, L., Kotlarski, S., Majone, B., Resch, G., Terzago, S., Valt, M., Beozzo, W., Cianfarra, P., Gouttevin, I., Marcolini, G., Notarnicola, C., Petitta, M., Scherrer, S.C., Strasser, U., Winkler, M., Zebisch, M., Cicogna, A., Cremonini, R., Debernardi, A., Faletto, M., Gaddo, M., Giovannini, L., Mercalli, L., Soubeyroux, J.-M., Sušnik, A., Trenti, A., Urbani, S., Weilguni, V., 2021. Observed snow depth trends in the European Alps: 1971 to 2019. The Cryosphere 15, 1343–1382. https://doi.org/10.5194/tc-15-1343-2021.